Journal of Multidisciplinary Engineering Science and Technology (JMEST)
ISSN: 2458-9403
Vol. 9 Issue 5, May - 2022

Determination Of Orbital Longitude Drift And Characterization Of The Operating Mean Orbital Longitude For Geostationary Satellites

Nnadi Nathaniel[1]
Cybersecurity Department, School of Information and Communication Technology,
Federal University of Technology Owerri.
nnadinathaniel2014@gmail.com

Young, Emem Godwin[2]
Department of Computer Engineering
Akwa Ibom State Polytechnic , Ikot Osurua Ikot Ekpene

Uduak Etim Udoka[3]
Department of Computer Engineering
Akwa Ibom State Polytechnic , Ikot Osurua Ikot Ekpene

***Abstract*— In this paper, determination of orbital longitude drift and characterization of the operating mean orbital longitude for a geostationary satellites is presented. Specifically, the MOLNIYA 1-S satellite with Norad catalogue number of 7392 was used as the case study satellite. The study determined the orbital longitude drift of the satellite from five different longitude datasets that were captured on different time of the day between 15th of July 2022 and 23rd of July 2022. The results showed that the orbital longitude drift was - 0.26467 °/day. The orbital longitude drift obtained in this paper compared very well with the value of 0.261°W degrees per day, which was published on http://www.satellite-calculations.com/ for the date 2022-07-15. In addition, a linear model was developed for predicting the effective population mean longitude for assessing the sample mean at any given date from the first data capture date. In all, it was found that due to the continues drift in the orbital longitude, a single value population mean is not good enough for assessing the sample mean of different datasets captured on different times.**

Keywords*— Orbital Longitude, Orbital Drift, MOLNIYA 1-S satellite, Mean Orbital Longitude, Geostationary Satellite

1. Introduction

Over the years, satellite applications has evolved and has become the bedrock of global communications, earth resource monitoring, geodesic processes, global positioning, military operations, world wide web, Internet of Things applications, among others [1,2, 3,4, 5,6, 7,8, 9, 10]. Application of satellites in all these areas requires accurate tracking of the satellites are they move in their orbits [11,12,13,14,15,16,17]. As such, proper determination of the orbital location of the satellites at any epoch is essential for satellite applications [18,19, 20,21, 22, 23, 24].

Notably, the geosynchronous (GEO) satellite, otherwise known as geostationary satellites are presumably fix at a given location at the equation and at a fixed longitude [25,26,27,28,29,30, 31, 32]. However, studies have shown that the GEO satellites do drift at certain rate with respect to their orbital longitude and latitude specifications [31,32, 33,34, 35,36, 37,38, 39,40, 41,42, 43, 44, 45]. The drift causes hourly and diurnal variations in the instantaneous orbital slot longitude and latitude of the satellites. As such, some online satellite tracking tool specify the hourly orbital location of the satellite along with the current drift value at any epoch. The drift parameter enables researchers to accurately determine the orbital slot parameters at any other epoch without recourse to the lengthy computation of the orbital slot from the Two Line Element (TLE) dataset [46,47,48,49,50].

Consequently, in this paper, the approach for the determination of the orbital drift and model for estimating the future orbital longitude of GEO satellite based on the current and historical satellite tracking dataset is presented. The t-test statistic is used to evaluate the orbital longitude dataset and also to evaluate the accuracy of the predicted future mean orbital longitude obtained from this paper [51,52,53,54,55]. The idea presented in this paper will help researchers to evaluate satellite prediction tool datasets and also learn how to effectively characterize the variations in the orbital slot longitude of GEO satellites.

2. Methodology

The case study satellites is MOLNIYA 1-S satellite with Norad catalogue number of 7392. The data driven analysis is based on the five datasets of 170 hours orbital longitude datasets of the case study satellite. The datasets were obtained from the online satellite tracking tool located at http://www.satellite-calculations.com/. The five datasets (shown in Figure 1 and Table 1) were captured on different time of the day between 15th of July 2022 and 23rd of July 2022.

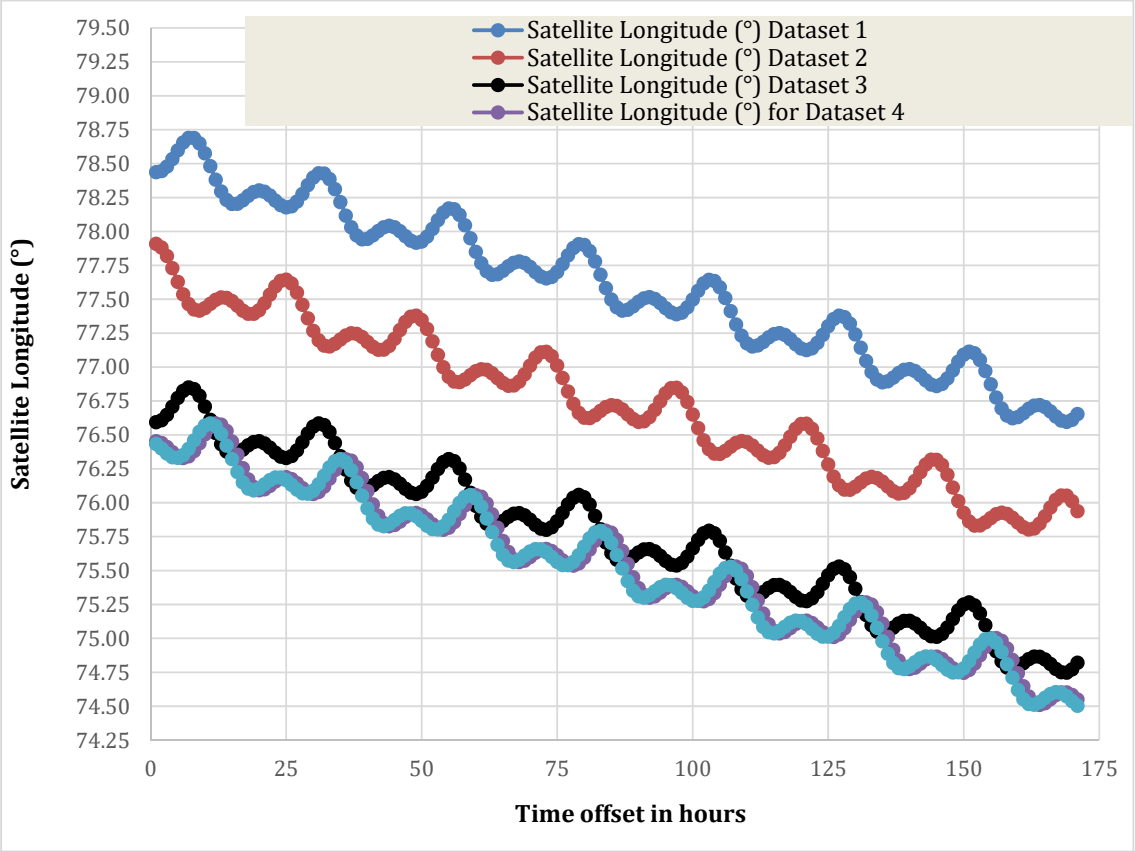

Figure 1 The graph of the satellite longitude versus time offset in hours for the five datasets of the orbital longitude of the cased study satellite

Table 1 The summary of the five longitude datasets captured for the case study satellite

	Dataset 1 captured on 7/15/2022 7:59	**Dataset 2 captured on 7/18/2022 14:32**	**Dataset 3 captured on 7/22/2022 7:55**	**Dataset 4 captured on 7/23/2022 2:48**	**Dataset 5 captured on 7/23/2022 4:07**
Minimum Longitude (°)	76.595	75.802	74.747	74.509	74.503
Maximum Longitude (°)	78.689	77.908	76.85	76.584	76.585
Range of Longitude (°)	2.094	2.106	2.103	2.075	2.082
Mean Longitude (°) denoted as $MLong_{(K)}$ where k = 1,2,3,4,5	77.59398246	76.73331579	75.74108772	75.53330409	75.51822222

The data capture time is first splits into day, hour and minutes, as shown in column 2, 3 and 4 of Table 2. Then, the data capture time is expressed in days, as shown in column 5 of Table 2. Particularly, let $Tdday_{(K)}$ denote the data capture time in day for dataset k, where k = 1,2,3,4,5 and $Tdhm_{(K)}$ denote the data capture time in day ($dy_{(k)}$), hour ($hr_{(k)}$) and minutes ($Mn_{(k)}$), then,

$$Tdday_{(K)} = dy_{(k)} + \frac{hr_{(k)}}{24} + \frac{Mn_{(k)}}{24*60} \quad \textbf{(1)}$$

In terms of the columns in Table 3, $Tdday_{(K)}$ = column 5, $dy_{(k)}$ = Column 2 , $hr_{(k)}$ =Column 3 and $Mn_{(k)}$ =Column 4 Hence;

$$\boldsymbol{Tdday_{(K)} = \text{Column 5} = Column\ 2 + \frac{Column\ 3}{24} + \frac{Column\ 4}{24*60}} \quad \textbf{(2)}$$

In Table 2, the first data capture was used as the starting point. Hence, the time interval between data capture started at 7/15/2022 7:59 (which is equivalent to 15.33263889 days). Hence, data capture in this case started at the 15.33263889 day. The next data capture was at18.60555556 day which gave time interval between data capture times of 3.272916667 days. This approach was used to determine the rest of the time interval between data capture times for the rest of the datasets. Specifically, if the time interval between data capture times in days for

dataset k is denoted as $TIntv_{(K)}$ where k = 1,2,3,4,5, then, accordingly,

$$TIntv_{(k)} = Tdday_{(K)} - TIntv_{(1)} \quad \textbf{(4)}$$

$$TIntv_{(1)} = 15.33263889 \quad \textbf{(3)}$$

Table 2 The detail for the computation of time interval between data capture times in days

Date and time of data capture	Data capture time in day, hour and minutes			Data capture time in days	Time interval between data capture times in days
	Day $[dy_{(k)}]$	Hour $[hr_{(k)}]$	Minutes $[Mn_{(k)}]$	Time in days $[Tdday_{(K)}]$	Time interval between data capture (days) $[TIntv_{(k)}]$
1	***2***	***3***	***4***	***5***	***6***
Formulas used				***(Column 2) + (Column 3 /24) + (Column 4 /(24 *60))***	***Column 5 - 15.33263889***
7/15/2022 7:59	15	7	59	15.33263889	0
7/18/2022 14:32	18	14	32	18.60555556	3.272916667
7/22/2022 7:55	22	7	55	22.32986111	6.997222222
7/23/2022 2:48	23	2	48	23.11666667	7.784027778
7/23/2022 4:07	23	4	7	23.17152778	7.838888889

Again, the mean of the first dataset was used as the reference mean value for modelling the longitudinal drift. Hence, a linear model used is given as;

$$\text{Mean Longitude } (°) = (M)\,(TIntv_{(k)}) + 77.59398 \quad (5)$$

Where M is the slope of the line and it represents the Longitude Drift in degrees/day while $TIntv_{(k)}$ is the time interval between data capture with unit as day.

3. Results and discussion

The results obtained for the time interval between data capture times (days) and the mean Longitude based on the five online datasets are given in Table 3 and Figure 2. From the results, the orbital longitude drift at this time is -0.26467 °/day. In essence, the mean longitude is reducing at - 0.26467 degrees per day. Also, the negative value means that the drift is westward. Hence, - 0.26467 degrees per day means 0.26467 west. The value of the orbital longitude drift obtained from http://www.satellite-calculations.com/Satellite/Catalog/catalogID.php?7392 on 2022-07-15 is 0.261°W [degrees per day].

Table 3 The time interval between data capture times (days) and the mean longitude (°) for the five datasets of the case study satellite

Time interval between data capture times (days) $TIntv_{(k)}$	Mean Longitude (°) from online datasets $MLong_{(K)}$
0	77.59398
3.272916667	76.73332
6.997222222	75.74109
7.784027778	75.5333
7.838888889	75.51822

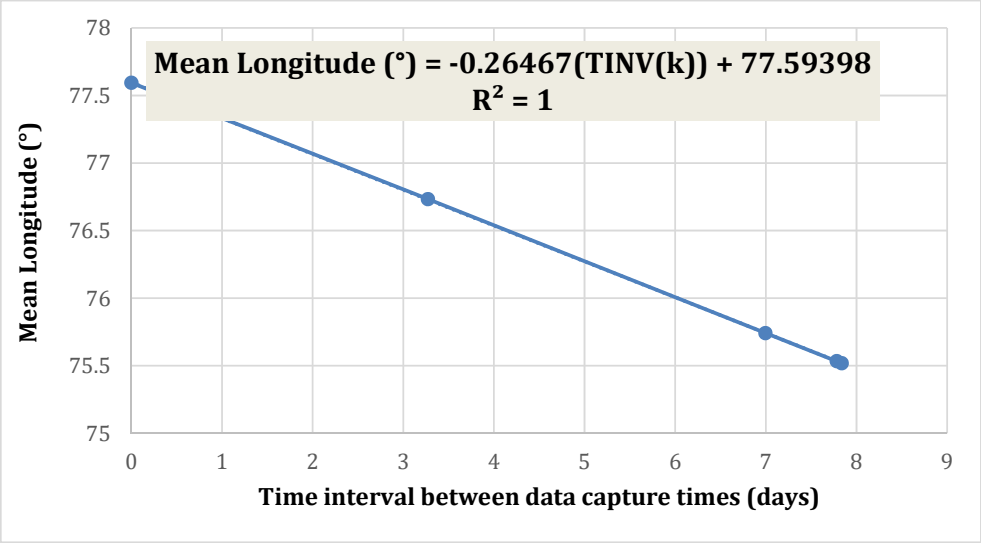

Figure 2 The graph plot of the time interval between data capture times (days) and the mean longitude (°) for the five datasets of the case study satellite

With the orbital longitude drift determined as -0.26467 degrees per day, the operating mean orbital longitude for the satellite can be predicted using the expression;

$$\text{Mean Orbital Longitude (°)} = -0.26467(TIntv_{(k)})) + 77.59398 \quad (6)$$

The results of the predicted operating mean orbital longitude are given in Table 4.

Table 4 The predicted operating mean orbital longitude

Date and time of data capture	Time interval between data capture (days)	Actual mean longitude (°) from online datasets	Predicted mean longitude (°)	Prediction Error (°)
7/15/2022 7:59	0	77.59398	77.59398	0
7/18/2022 14:32	3.272916667	76.73332	76.72773	0.005586114
7/22/2022 7:55	6.997222222	75.74109	75.74202	-0.000928225
7/23/2022 2:48	7.784027778	75.5333	75.53377	-0.000473615
7/23/2022 4:07	7.838888889	75.51822	75.51925	-0.00103347
			RMSE	0.002582969

The t-test analysis of the first dataset and the second dataset based on the common population mean longitude of 77.59° are shown in Figure 3 and Figure 4 respectively. Again, the summary of the t-test analysis results for the five datasets based on the common population mean longitude of 77.59° are shown in Table 5 and Figure 5. The results in Table 5 show that only the first dataset has sample mean that conforms with the population mean.

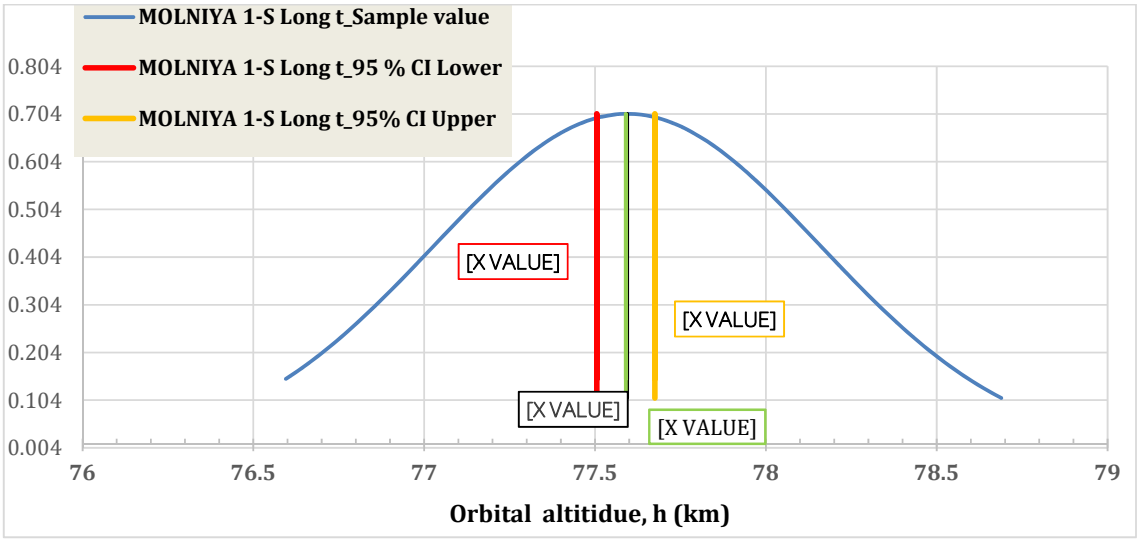

Figure 3 The t-test analysis of the first dataset based on the common population mean longitude of 77.59°

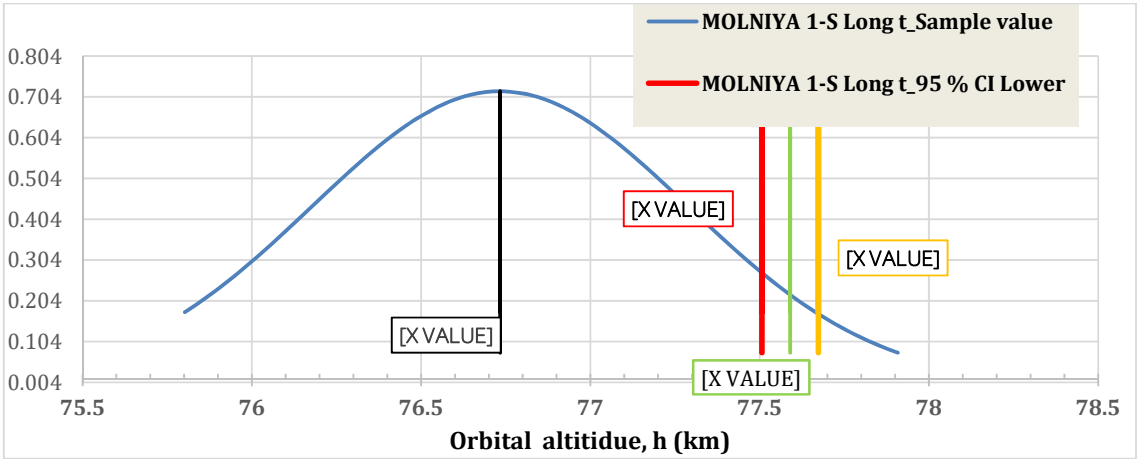

Figure 4 The t-test analysis of the second dataset based on the common population mean longitude of 77.59°

Table 5 The summary of the t-test analysis results for the five datasets based on the common population mean longitude of 77.59°

	Dataset 1	Dataset 2	Dataset 3	Dataset 4	Dataset 5
Dataset Mean Longitude (°)	77.5940	76.7333	75.7411	75.5333	75.5182
Satellite orbital Longitude (°)	77.59	77.59	77.59	77.59	77.59
95% CI, lower value	77.5050	77.5066	77.5048	77.5056	77.5054
95% CI, upper value	77.6750	77.6734	77.6752	77.6744	77.6746
Comment	Dataset 1 Mean is within the CI range. It means the sample data mean longitude is the same as the accepted mean orbital longitude	Dataset 2 Mean is outside the CI range. It is smaller than the lower value of the CI	Dataset 3 Mean is outside the CI range. It is smaller than the lower	Dataset 4 Mean is outside the CI range. It is smaller than the lower	Dataset 5 Mean is outside the CI range. It is smaller than the lower

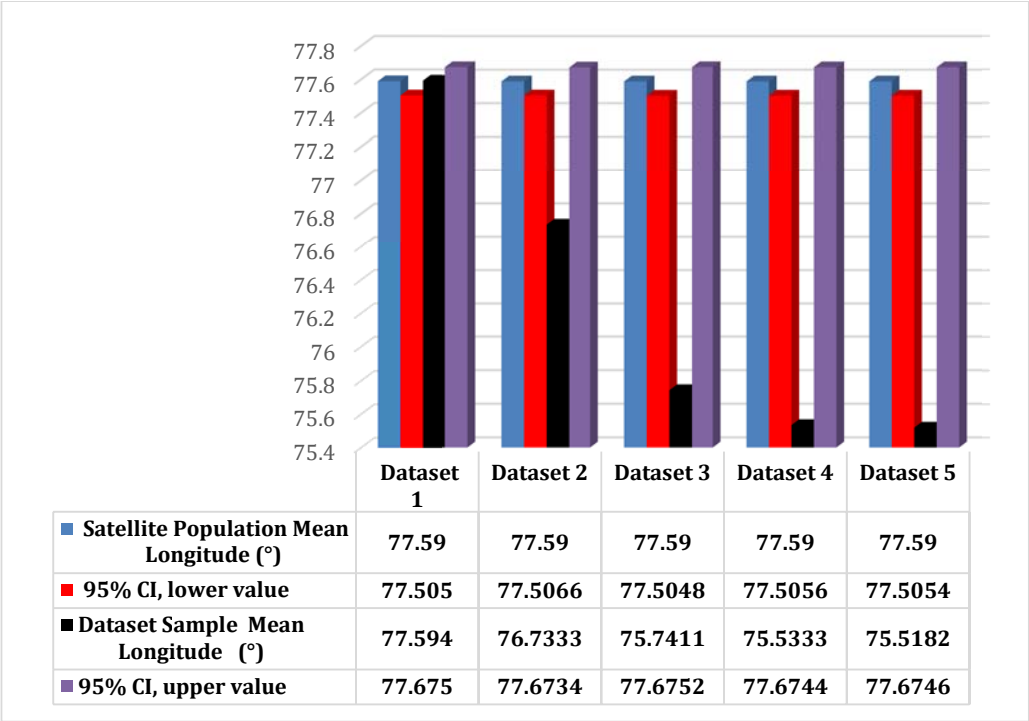

	Dataset 1	Dataset 2	Dataset 3	Dataset 4	Dataset 5
Satellite Population Mean Longitude (°)	77.59	77.59	77.59	77.59	77.59
95% CI, lower value	77.505	77.5066	77.5048	77.5056	77.5054
Dataset Sample Mean Longitude (°)	77.594	76.7333	75.7411	75.5333	75.5182
95% CI, upper value	77.675	77.6734	77.6752	77.6744	77.6746

Figure 5 The bar chat of the t-test analysis results for the five datasets based on the common population mean longitude of 77.59°

The t-test analysis of the second dataset and the third dataset based on the predicted population mean longitude are shown in Figure 6 and Figure 7 respectively. Again, the summary of the t-test analysis results for the five datasets based on the predicted population mean longitude for each of the five datasets are shown in Table 6 and Figure 8. The results in Table 6 show that all the five datasets has sample mean that conforms with the population mean.

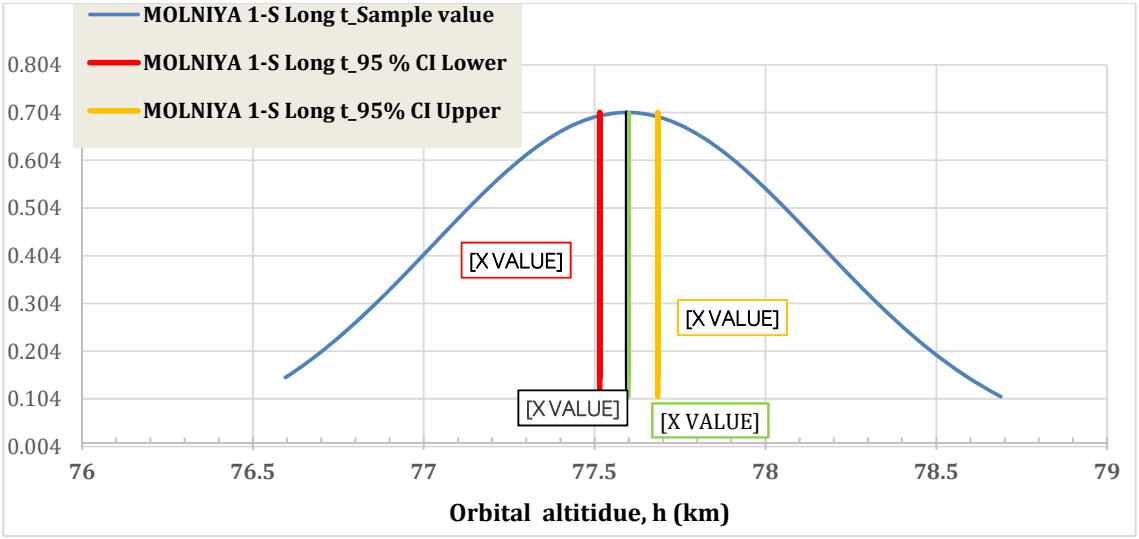

Figure 6 The t-test analysis of the second dataset based on the predicted population mean longitude 77.6°

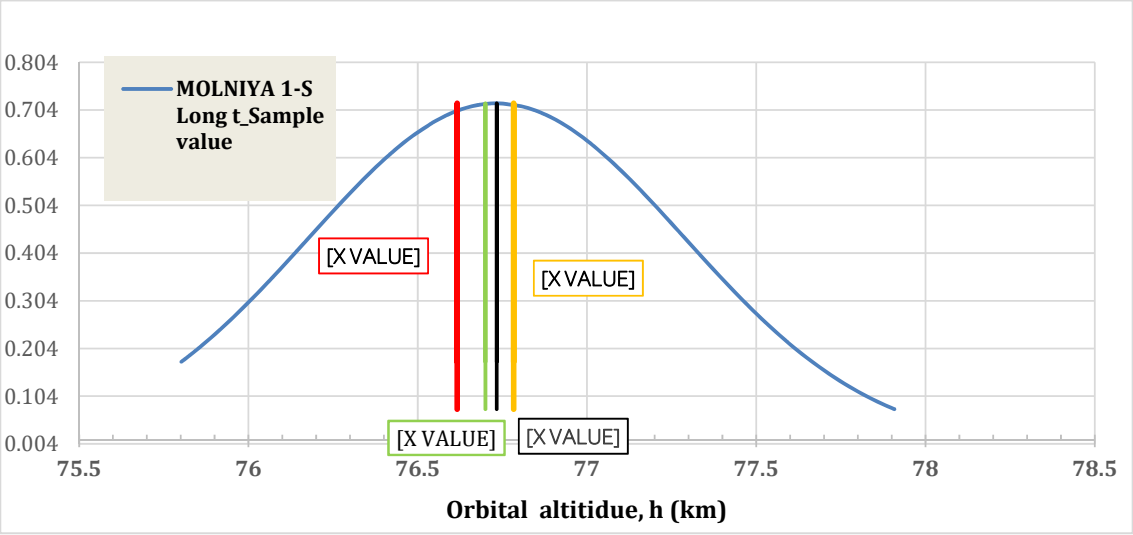

Figure 7 The t-test analysis of the second dataset based on the the predicted population mean longitude 77.7°

Table 6 The summary of the t-test analysis results for the five datasets based on the predicted population mean longitude for each of the five datasets

	Dataset 1	Dataset 2	Dataset 3	Dataset 4	Dataset 5
Sample Mean Longitude (°)	77.5940	76.7333	75.7411	75.5333	75.5182
Population Mean Longitude (°)	77.6	76.7	75.7	75.5	75.5
95% CI, lower value	77.5150	76.6166	75.6148	75.4156	75.4154
95% CI, upper value	77.6850	76.7834	75.7852	75.5844	75.5846
Comment	Dataset 1 Mean is within the CI range. It means the sample data mean longitude is the same as the accepted mean orbital longitude	Dataset 2 Mean is within the CI range. It means the sample data mean longitude is the same as the accepted mean orbital longitude	Dataset 3 Mean is within the CI range. It means the sample data mean longitude is the same as the accepted mean orbital longitude	Dataset 4 Mean is within the CI range. It means the sample data mean longitude is the same as the accepted mean orbital longitude	Dataset 5 Mean is within the CI range. It means the sample data mean longitude is the same as the accepted mean orbital longitude

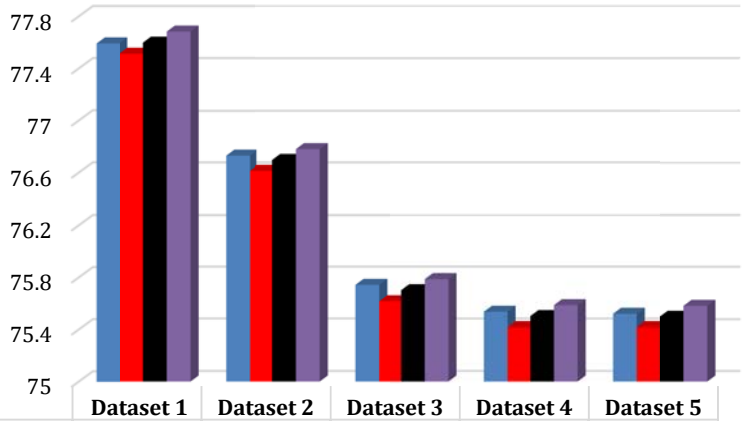

	Dataset 1	Dataset 2	Dataset 3	Dataset 4	Dataset 5
Dataset Sample Mean Longitude (°)	77.594	76.7333	75.7411	75.5333	75.5182
95% CI, lower value	77.515	76.6166	75.6148	75.4156	75.4154
Satellite Population Mean Longitude (°)	77.6	76.7	75.7	75.5	75.5
95% CI, upper value	77.685	76.7834	75.7852	75.5844	75.5846

Figure 8 The bar chat of the t-test analysis results for the five datasets based on the predicted population mean longitude for each of the five datasets

4. Conclusion

The effect of drift in the orbital longitudinal of Molniya satellite is examined. The t-test statistics was used to evaluate if the sample mean of different datasets captured at different times conforms to a common population mean that is subjected to the drift. Furthermore, the prediction model was developed for estimating the running population mean with respect to the drift. In all, it was found that a single value population mean is not good enough for assessing the sample mean of different datasets captured on different times.

References

1. Ryerson, R. A., & CMS, F. (2015). *Global navigation satellite system augmentation models environmental scan*. Natural Resources Canada.
2. Khan, A., Gupta, S., & Gupta, S. K. (2020). Multi-hazard disaster studies: Monitoring, detection, recovery, and management, based on emerging technologies and optimal techniques. *International journal of disaster risk reduction*, *47*, 101642.
3. Lillesand, T., Kiefer, R. W., & Chipman, J. (2015). *Remote sensing and image interpretation*. John Wiley & Sons.
4. Dixon, B., & Uddameri, V. (2016). *GIS and geocomputation for water resource science and engineering*. John Wiley & Sons.
5. Clark, R. M. (2020). *Geospatial Intelligence: Origins and Evolution*. Georgetown University Press.
6. Sofia, G. (2020). Combining geomorphometry, feature extraction techniques and Earth-surface processes research: The way forward. *Geomorphology*, *355*, 107055.
7. Gaffey, C., & Bhardwaj, A. (2020). Applications of unmanned aerial vehicles in cryosphere: Latest advances and prospects. *Remote Sensing*, *12*(6), 948.
8. Othman, E. S. M. E. A. (2022). *Data Communication Enhancement for the Egyptian Coast Monitoring System* (Doctoral dissertation, Faculty of Engineering, Minia University).
9. Davidson-Arnott, R., Bauer, B., & Houser, C. (2019). *Introduction to coastal processes and geomorphology*. Cambridge university press.
10. Labi, S. (2014). *Introduction to civil engineering systems: A systems perspective to the development of civil engineering facilities*. John Wiley & Sons.
11. Hu, Y., Bai, X., Chen, L., & Yan, H. (2019). A new approach of orbit determination for LEO satellites based on optical tracking of GEO satellites. *Aerospace Science and Technology*, *84*, 821-829.
12. Mjelde, A., Martinsen, K., Eide, M., & Endresen, Ø. (2014). Environmental accounting for Arctic shipping–a framework building on ship tracking data from satellites. *Marine pollution bulletin*, *87*(1-2), 22-28.
13. Elbeltagy, A. E. H. M., Youssef, A. M., Bayoumy, A. M., & Elhalwagy, Y. Z. (2018). Fixed ground-target tracking control of satellites using a nonlinear model predictive control.

14. Zheng, Y., Ganushkina, N. Y., Jiggens, P., Jun, I., Meier, M., Minow, J. I., ... & Kuznetsova, M. M. (2019). Space radiation and plasma effects on satellites and aviation: Quantities and metrics for tracking performance of space weather environment models. *Space Weather*, *17*(10), 1384-1403.
15. Scanlon, B. R., Zhang, Z., Rateb, A., Sun, A., Wiese, D., Save, H., ... & Reedy, R. C. (2019). Tracking seasonal fluctuations in land water storage using global models and GRACE satellites. *Geophysical Research Letters*, *46*(10), 5254-5264.
16. Zarei, S., Bakhtiari, M., & Daneshjou, K. (2021). Relative attitude tracking of two satellites in the presence of third-body perturbation and considering actuator saturation. *Journal of the Brazilian Society of Mechanical Sciences and Engineering*, *43*(12), 1-15.
17. Peckham, R., & Sinha, R. (2017). Satellites and the new war on infection: tracking Ebola in West Africa. *Geoforum*, *80*, 24-38.
18. Zhang, R., Zhang, Q., Huang, G., Wang, L., & Qu, W. (2015). Impact of tracking station distribution structure on BeiDou satellite orbit determination. *Advances in Space Research*, *56*(10), 2177-2187.
19. Zehentner, N., & Mayer-Gürr, T. (2016). Precise orbit determination based on raw GPS measurements. *Journal of Geodesy*, *90*(3), 275-286.
20. Giordano, P., Zoccarato, P., Otten, M., & Crisci, M. (2017, September). P2OD: real-time precise onboard orbit determination for LEO satellites. In *Proceedings of the 30th International Technical Meeting of the Satellite Division of The Institute of Navigation (ION GNSS+ 2017)* (pp. 1754-1771).
21. Foster, C., Hallam, H., & Mason, J. (2015). Orbit determination and differential-drag control of Planet Labs CubeSat constellations. *arXiv preprint arXiv:1509.03270*.
22. Corbett, H., Law, N. M., Soto, A. V., Howard, W. S., Glazier, A., Gonzalez, R., ... & Quimby, R. (2020). Orbital foregrounds for ultra-short duration transients. *The Astrophysical Journal Letters*, *903*(2), L27.
23. Bidikar, B., Rao, G. S., Ganesh, L., & Kumar, M. S. (2014). Satellite clock error and orbital solution error estimation for precise navigation applications. *Positioning*, *2014*.
24. Steigenberger, P., Hugentobler, U., Loyer, S., Perosanz, F., Prange, L., Dach, R., ... & Montenbruck, O. (2015). Galileo orbit and clock quality of the IGS Multi-GNSS Experiment. *Advances in Space Research*, *55*(1), 269-281.
25. Schnecker Sr, J. F., Byrtus, B., Yang-Tsui, J., Jaime, B., Leary, E., & Luo, K. (2022). *Satellite-based Positioning, Navigation, and Timing (PNT)*. Naval Information Warfare Center Pacific.
26. Huffman, G. J., Bolvin, D. T., Nelkin, E. J., & Tan, J. (2015). Integrated Multi-satellitE Retrievals for GPM (IMERG) technical documentation. *Nasa/Gsfc Code*, *612*(47), 2019.
27. Elbert, B. (2014). *The satellite communication ground segment and earth station handbook*. Artech House.
28. Kuismanen, S. (2019). *Vulnerability of Mobile Phones to Navigation Signal Spoofing* (Master's thesis).
29. Minelli, G. (2018). *Resource Constrained Autonomous Operations Of Satellite Constellations And Ground Station Networks*. Naval Postgraduate School Monterey United States.
30. Rosengren, A. J. (2014). *Long-Term Dynamical Behavior of Highly Perturbed Natural and Artificial Celestial Bodies* (Doctoral dissertation, University of Colorado at Boulder).
31. Khan, M. R. H., Ziad, M. O., Chowa, S. M., & Mehedi, M. (2021). *A comparative study of intelligent reflecting surface and relay in satellite communication* (Doctoral dissertation, Brac University).
32. Wang, N., Yuan, Y., Li, Z., Montenbruck, O., & Tan, B. (2016). Determination of differential code biases with multi-GNSS observations. *Journal of Geodesy*, *90*(3), 209-228.
33. Weiss, A., Kalabić, U. V., & Di Cairano, S. (2018). Station keeping and momentum management of low-thrust satellites using MPC. *Aerospace Science and Technology*, *76*, 229-241.
34. Huang, X., Yang, B., Li, S., & Wang, Z. (2021). Efficient high-accuracy north-south station-keeping strategy for geostationary satellites. *Science China Technological Sciences*, *64*(11), 2415-2426.
35. Guelman, M. M. (2014). Geostationary satellites autonomous closed loop station keeping. *Acta Astronautica*, *97*, 9-15.
36. Gazzino, C., Louembet, C., Arzelier, D., Jozefowiez, N., Losa, D., Pittet, C., & Cerri, L. (2017). Integer programming for optimal control of geostationary station keeping of low-thrust satellites. *IFAC-PapersOnLine*, *50*(1), 8169-8174.

37. Borissov, S., Wu, Y., & Mortari, D. (2015). East–west GEO satellite station-keeping with degraded thruster response. *Aerospace*, *2*(4), 581-601.
38. Li, L., Zhang, J., Li, Y., & Zhao, S. (2019). Geostationary station-keeping with electric propulsion in full and failure modes. *Acta Astronautica*, *163*, 130-144.
39. Yuxin, L. I. U., Haibin, S. H. A. N. G., & Shuai, W. A. N. G. (2015). Research on GEO satellite station keeping method using electric propulsion. *深空探测学报 (中英文)*, *2*(1), 80-87.
40. Gazzino, C., Arzelier, D., Losa, D., Louembet, C., Pittet, C., & Cerri, L. (2016). Optimal control for minimum-fuel geostationary station keeping of satellites equipped with electric propulsion. *IFAC-PapersOnLine*, *49*(17), 379-384.
41. Nicolás-Álvarez, J., Carreño-Megias, X., Fusté, O., Ferrer, E., Albert, M., Amlou, A., ... & Broquetas, A. (2021, July). Station-Keeping Manoeuvre Detection for Autonomous Precise Interferometric Tracking of Geosynchronous Satellites. In *2021 IEEE International Geoscience and Remote Sensing Symposium IGARSS* (pp. 7783-7786). IEEE.
42. Skinner, M. A., Russell, R. W., Kelecy, T., Gregory, S., Rudy, R. J., Kim, D. L., & Crawford, K. (2014). Observations in the thermal IR and visible of a retired satellite in the graveyard orbit, and comparisons to active satellites in GEO. *Acta Astronautica*, *105*(1), 1-10.
43. Li, L., Gkolias, I., Colombo, C., & Zhang, J. (2019). Design of low-thrust control in the geostationary region for station keeping.
44. Zou, H., Song, J., Wang, J., Zhang, L., & Huang, Y. (2020, August). Geostationary Station Keeping Using Relative Orbital Elements with Model Predictive Control. In *2020 Chinese Control And Decision Conference (CCDC)* (pp. 4437-4442). IEEE.
45. Li, L., Zhang, J., Gkolias, I., & Colombo, C. (2019, July). Constellation Design and Low-Thrust Station-Keeping Strategy for Satellites in Inclined Geosynchronous Orbits. In *2019 IEEE 10th International Conference on Mechanical and Aerospace Engineering (ICMAE)* (pp. 108-114). IEEE.
46. Shi, C., Li, W., Li, M., Zhao, Q., & Sang, J. (2015). Calibrating the scale of the NRLMSISE00 model during solar maximum using the two line elements dataset. *Advances in Space Research*, *56*(1), 1-9.
47. Bai, X., Liao, C., Pan, X., & Xu, M. (2019). Mining two-line element data to detect orbital maneuver for satellite. *IEEE Access*, *7*, 129537-129550.
48. Roberts, T. G., & Linares, R. (2020). Satellite Repositioning Maneuver Detection in Geosynchronous Orbit Using Two-line Element (TLE) Data. In *International Astronautical Congress*.
49. Lemmens, S., & Krag, H. (2014). Two-line-elements-based maneuver detection methods for satellites in low earth orbit. *Journal of Guidance, Control, and Dynamics*, *37*(3), 860-868.
50. Speretta, S., Sundaramoorthy, P., & Gill, E. (2017, April). Long-term performance analysis of NORAD Two-Line Elements for CubeSats and PocketQubes. In *11th IAA Symposium on Small Satellites for Earth Observation* (pp. 1-6). DLR.
51. Gravetter, F. J., & Wallnau, L. B. (2014). Introduction to the t statistic. *Essentials of statistics for the behavioral sciences*, *8*, 252.
52. Kim, T. K. (2015). T test as a parametric statistic. *Korean journal of anesthesiology*, *68*(6), 540-546.
53. Hedberg, E. C., & Ayers, S. (2015). The power of a paired t-test with a covariate. *Social science research*, *50*, 277-291.
54. Xu, M., Fralick, D., Zheng, J. Z., Wang, B., & Changyong, F. E. N. G. (2017). The differences and similarities between two-sample t-test and paired t-test. *Shanghai archives of psychiatry*, *29*(3), 184.
55. Kim, T. K., & Park, J. H. (2019). More about the basic assumptions of t-test: normality and sample size. *Korean journal of anesthesiology*, *72*(4), 331-335.